Hindawi
Wireless Communications and Mobile Computing
Volume 2022, Article ID 9167017, 15 pages
https://doi.org/10.1155/2022/9167017

Research Article

Optimization of Rolling Schedule for Single-Stand Reversible Cold Rolling Mill Based on Multiobjective Artificial Fish Swarm Algorithm

Zhe Yang[1,2], **Ding Liu**[1,2], **Xinyu Zhang**[1,2], **Weichao Huang**[1,2] and **Gang Zheng**[1,2]

[1]*Faculty of Automation and Information Engineering, Xi'an University of Technology, Xi'an 710048, China*
[2]*Shaanxi Key Laboratory of Complex System Control and Intelligent Information Processing, Xi'an University of Technology, Xi'an 710048, China*

Correspondence should be addressed to Zhe Yang; yangzhex@126.com

Received 5 August 2022; Revised 29 August 2022; Accepted 30 August 2022; Published 16 September 2022

Academic Editor: Mingqian Liu

The single-stand reversible cold rolling mill is important equipment in the production of steel strips. The rolling schedule is the core technological content in the strip production of the single-stand reversible cold rolling mill. The scientific rolling schedule is the fundamental guarantee for the production capacity of the rolling mill, product quality, accuracy, shape quality, energy saving, and consumption reduction. This paper takes the dynamic rolling process of single-stand cold rolling as the research object, the purposes of increasing production capacity, saving energy, and reducing consumption are achieved by optimizing the rolling schedule. Based on the study of the mechanism model and the analysis of a large number of field measured data, a slice of mathematical models of the rolling process suitable for engineering calculation are proposed, and a few objective functions suitable for the single-stand reversible cold rolling process are designed. On this basis, the artificial fish swarm algorithm is improved into a multiobjective optimization algorithm for the optimization of rolling schedule, and the optimal rolling load distribution scheme is obtained. Finally, the optimization method of rolling schedule proposed in this paper is applied to the actual rolling production. The results show that the proposed method can improve productivity and save energy compared with the empirical rolling schedule, and the feasibility and validity of the proposed algorithm are verified.

1. Introduction

The cold-rolled sheets and strips are an important steel product for iron and steel enterprises, and it is also the product with the highest technical content in iron and steel products. It is widely used in automobiles, ship, construction, home appliances, light industry, machinery manufacturing, chemicals, hardware products, and packaging industries. The single-stand reversible cold rolling mill is important equipment for steel sheet and strip production. Although, compared with the tandem cold rolling mill, the single-stand reversible cold rolling mill has the disadvantages of low production efficiency and low yield, but the advantage of it is that the production method is relatively flexible, suitable for the production of ultrathin strip steel, low investment, and can produce a variety of small batches of products of different specifications. Therefore, the single-stand reversible cold rolling mill has an irreplaceable role. With the continuous improvement of the quality requirements of cold-rolled products and the pressure of cost, environmental protection, market, and other aspects, the production of modern single-stand reversible cold-rolling mills has the extreme pursuit of high precision, high yield, high production efficiency, and low production cost. In this case, for the single-stand cold rolling mill, in addition to improving the control accuracy of the automatic control system through advanced control methods, the rolling process is also put forward with higher requirements. Rolling

schedule is the core process technology in rolling production, which has a significant impact on production, quality, cost, production safety, and process control accuracy. Reasonable rolling schedule can not only improve the productivity of strip steel, reduce energy consumption but also ensure product quality, improve process control accuracy, response speed, equipment utilization efficiency, and bring great economic benefits.

The cold rolling process has a complex mechanism, with typical characteristics of multivariable, strong coupling, nonlinear, and time-varying, it is very difficult to calculate accurately. Therefore, the traditional main methods of rolling schedule design are empirical form method, energy consumption curve method, and load distribution method based on rolling theory.

The empirical form method refers to the method of directly assigning the reduction amount and thickness of each pass or stand through the operator's production experience, and recording this experience through a table to form a standard rolling specification table as the basis for load distribution. The most significant advantage of the empirical form method is that it is easy to use and does not require complex theoretical calculations and machine operations [1]. At present, this method is still used in many steel companies. However, the empirical form method completely relies on the operator's experience, and it may not be optimal with the change of production conditions.

The energy consumption curve method is drawing the relationship between the power required for rolling a unit mass of rolled pieces and the thickness or elongation according to the historical rolling data. Since the inlet thickness and target thickness of the rolled piece have been determined, the total rolling power can be calculated from the energy consumption curve. On the premise that the load distribution ratio of each pass is known, the intermediate thickness of each pass can be derived according to the energy consumption curve, it means the reduction amount distribution scheme can be determined. This method has a long history of application and has been applied in hot tandem rolling as early as 1964 [2]. This method is effective when rolling strips of the same specification, but it is difficult to guarantee the rolling accuracy once the specification is changed, and it is necessary to repeat the experiment to draw the curve.

The load distribution method based on the rolling theory is to give full play to the production capacity of the rolling mill and prevent the overload of the mill load, so that the ratio between the production load and the limit load of each pass is constant, which is also called the load proportionality principle. The load value (reduction rate, rolling force, and motor power) of each pass can be calculated according to the relevant rolling mathematical model. Furthermore, the target thickness for each pass is obtained by solving a set of nonlinear equations. The Newton-Raphson method was used to solve the nonlinear equation system [3], but this method needs to solve the inverse of the Jacobian matrix and the reciprocal of the rolling load to the thickness, which is complicated to calculate and sensitive to the initial value [4]. Many scholars have improved this method and reduced the amount of computation [5, 6]. However, the load distribution method based on rolling theory still cannot get rid of the dependence of artificial experience.

To get rid of the influence of empirical values, optimization techniques are introduced into rolling schedule optimization. Especially, with the improvement of industrial computer performance, many single-objective and multiobjective intelligent optimization algorithms have been applied to rolling schedule design in recent years, and various objective functions have been established for different technological objectives. Because of the high efficiency and fast running speed, the rolling schedule design based on single objective optimization algorithm has been widely used in practical production. Jin et al. designed the load distribution using a genetic algorithm method with excellent flatness as the objective function [7]. Cao et al. used the self-adaptive particle swarm optimization algorithm to design the load distribution model [8]. With the increasing requirements of rolling production, the increasing factors need to be considered, and the results of load distribution according to a single objective function are difficult to fully meet the various requirements of the rolling process. Therefore, multiobjective optimization methods are gradually introduced into rolling schedule design. The optimization method of multiobjective rolling schedule is divided into a priori method and a posteriori method. In the priori method, the multiobjective optimization problem is transformed into a single-objective optimization problem by means of a weighted sum. Yang et al. used a set of fixed weight coefficients to convert the motor power consumption objective function and the slip prevention objective function into a comprehensive objective function and optimized the rolling schedule through an improved artificial bee colony algorithm based on chaos theory [9]. Chen et al. proposed a schedule optimization model based on cost functions, which take rolling force, motor power, interstand tension, and stand reduction into consideration, and the Nelder-Mead simplex method was used to optimize the rolling schedule [10]. Bu et al. transformed the power objective function, tension objective function, and flatness objective function into a comprehensive objective function through the influence function, and the Tabu search algorithm was used to optimize the rolling schedule [11]. Wang et al. designed a dynamic adjustment model for the weight coefficients of objectives based on rolling length and used NSGA-II to optimize the rolling schedule [12]. The difficulty of the a priori method lies in the determination of the weight coefficient, and the choice of the weight coefficient directly affects the optimization effect. Compared with the prior method, the posterior method is more suitable for practical applications. The posterior method obtains a set of complementary dominant Pareto solution set for selecting according to the actual requirements without setting weight coefficients. Che et al. used the chaotic multiobjective quantum genetic algorithm to optimize the rolling schedule with the equal relative load and flatness of the last stand as the objective functions [13]. Li and Fang designed a robust multiobjective optimization model of rolling schedule for tandem cold rolling and proposed a differential evolution algorithm based on the evolutionary direction [14]. Wei et al. used an improved

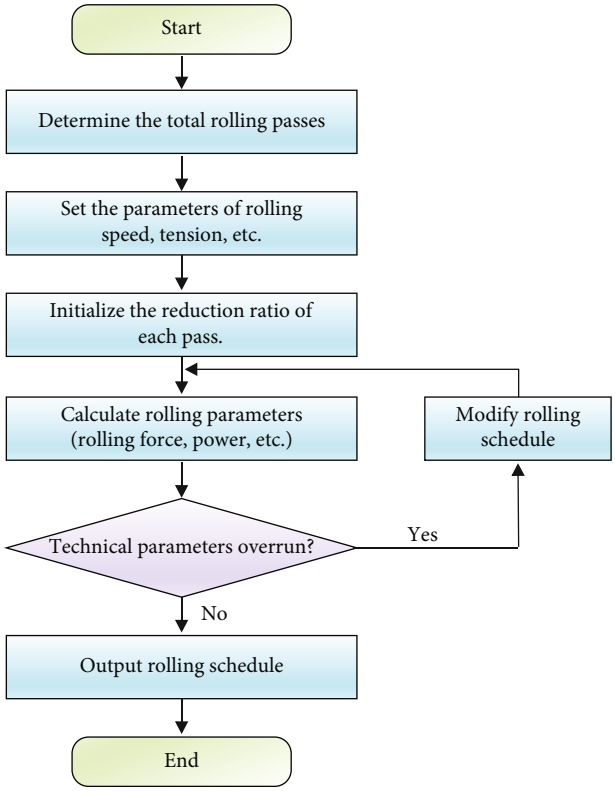

Figure 1: The flow chart of rolling schedule design of single-stand reversible cold rolling mill.

multiobjective particle swarm algorithm to optimize the objective functions of equal relative load and slip rate, and the method was applied to a five-stand tandem mill [15]. Wang et al. proposed a multiobjective particle swarm optimizer with dynamic opposition-based learning to optimize the rolling schedule with the objectives of minimum energy consumption, relative power margin, and slippage preventing [16]. Hu et al. selected five objectives as optimization objectives and used a multiobjective evolutionary algorithm based on decomposition and Gaussian mixture model to design the rolling schedule [17]. Taking the practical engineering application as the starting point, Zoheir et al. used the NSGA-II algorithm to realize the optimization of the rolling schedule of the tandem mill, and fully compared with the optimization results of the single-objective rolling schedule and the original rolling schedule [18]. At present, the main research is on the optimization of rolling schedule for continuous rolling mills, and the optimization of multiobjective rolling schedules for single-stand cold rolling mills is less. How to give full play to the advantages of the multiobjective optimization algorithm in the optimization of the rolling schedule of the single-stand rolling mill still needs to be further research.

In this paper, a rolling schedule optimization method based on multiobjective artificial fish swarm algorithm is developed to solve the rolling schedule optimization problem of single stand reversing cold mill. The major works of this paper are as follows:

(1) The related problems of multiobjective optimization of rolling schedule for single-stand cold rolling mill are discussed

(2) A few of the mathematical models of the rolling process of single-stand cold rolling mill suitable for practical engineering applications are proposed

(3) The artificial fish swarm algorithm is improved into a multiobjective optimization method and applied to the rolling schedule optimization

(4) The proposed method is verified by practical engineering application, and the results are satisfactory

The remainder of this paper is organized as follows: Section 2 discusses the related problems of the design of rolling schedule and gives a mathematical model of rolling process suitable for engineering applications. The basic theory of artificial swarm algorithm and the detail of the proposed method are introduced in Section 3. Section 4 makes the application and verification of the proposed method in the practical rolling project. Section 5 contains some conclusions plus some ideas for further work.

2. Problems Related to the Optimization of Rolling Schedule

The technological characteristic of rolling production of single-stand reversible cold rolling mill is that the raw material of the steel strip undergoes reciprocating rolling in multiple passes and finally reaches the finished product thickness. The design of rolling schedule is assigning the rolling technological parameters according to the rolling strategy and the rolling mathematical model, including rolling pass, pass reduction, rolling force, front and back tension, and rolling speed. For a single-stand reversing cold rolling mill, the pass reduction is the most important technological parameter. The distribution of the rolling reduction of each pass constitutes the load distribution scheme. After the load distribution scheme is determined, it will directly lead to the determination of rolling force, rolling power, and rolling speed according to the rolling mathematical model. Therefore, the optimization of the rolling schedule of the single-stand reversing cold rolling mill is mainly the optimization of the load distribution. According to setting the specific optimization objective, the optimal load distribution scheme is obtained by the optimization algorithm, and other rolling technological parameters are then calculated. Figure 1 shows the flow chart of the design of the rolling schedule for a single-stand reversing cold mill. The design and optimization of the rolling schedule is also one of the core functions of the rolling process automation system, and its role is to provide the reasonable preset values for the basic automation system. It can be seen that the optimization of the rolling schedule involves three problems: the mathematical model of the rolling process, the objective functions, and the optimization method.

2.1. The Main Mathematical Model of the Rolling Process. Mathematical models are the basis for rolling schedule design and the important basis for calculating the objective functions. The mathematical models required for the design of the rolling schedule of single-stand reversible rolling mill include rolling force model, deformation resistance model, friction coefficient model, forward slip model, tension model, rolling torque and power model, and rolling pass model. Among them, the most important is the rolling force model and the model related to the rolling force.

2.1.1. Rolling Force Model. The cold rolling process has a complex mechanism, with typical characteristics of multivariable, strong coupling, nonlinear, and time-varying, it is very difficult to obtain an accurate rolling force model. For decades, many scholars have conducted very detailed research and analysis on the cold rolling force model and obtained many cold rolling force models. Combined with the real-time calculation and practical engineering application experience, this paper chooses the Bland-Ford-Hill formula to calculate the rolling force.

$$\begin{cases} F = Bl' K_T Q_P K, \\ l' = \sqrt{R'\Delta h}, \\ R' = R\left(1 + 2.11 \times 10^{-5} \dfrac{F}{B\Delta h}\right), \\ Q_P = 1.08 + 1.79\mu\varepsilon\sqrt{1-\varepsilon}\sqrt{R'/h_1} - 1.02\varepsilon, \\ K_T = 1 - \dfrac{\tau_b + \tau_f}{2K}, \end{cases} \tag{1}$$

where F is the rolling force; B is the width of the steel strip; l' is the contact arc length of the rolled piece in the deformation zone during rolling; R is the roll radius; R' is the roll flattening radius; Q_P is the external friction stress state coefficient after flattening; K_T is the tension influence coefficient; K is the deformation resistance of steel strip; μ is friction coefficient; Δh is absolute reduction; τ_f is front tensile stress; τ_b is back tensile stress; ε is the reduction rate, i.e., the reduction rate $\varepsilon = (h_0 - h_1)/h_0$; h_1 is outlet thickness per pass; and h_0 is inlet thickness per pass. Friction coefficient μ and deformation resistance K are variables that cannot be measured by sensors, the calculation methods of these two parameters will be introduced in subsequent chapters.

2.1.2. Friction Coefficient Model. Because of constantly changing during the production process, the friction coefficient is very difficult to be calculated directly. In this paper, a friction coefficient calculation formula is proposed by analyzing and regressing the actual production data.

$$\mu = \mu_{basic} + \mu_{vl}, \tag{2}$$

where μ_{basic} is the basic friction coefficient model obtained by inversion of the Stone rolling force formula; and μ_{vl} is the correction factor related to the rolling speed and the rolling length of the roll.

$$\mu_{basic} = \frac{1/2\sqrt{\Delta h/R'}}{1 - 2\sqrt{(1-\varepsilon)(f/\varepsilon)}}, \tag{3}$$

where f is the forward slip, the calculation model of which is as follows:

$$\begin{gathered} f = \frac{R}{h_1}\gamma^2, \\ \gamma = \sqrt{\frac{h}{R}} \tan\left[\frac{1}{2}\arctan^{-1}\sqrt{\frac{\varepsilon}{1-\varepsilon}} + \frac{\pi}{8}\ln(1-\varepsilon)\sqrt{\frac{h}{R}}\right], \end{gathered} \tag{4}$$

where γ is the neutral angle of which is as follows:

$$\begin{gathered} \mu_{vl} = \frac{f(v)}{1 + g \cdot L/L_0}, \\ f(v) = av + bv^2 + cv^3 + dv^4 + ev, \end{gathered} \tag{5}$$

where L_0 is the benchmark rolling length$(1000m)$; v is the rolling speed; L is the cumulative rolling length after roll change; $f(v)$ is a predicted value of the friction coefficient depending on the speed, a, b, c, d, e are polynomial regression coefficients; and g is a coefficient related to rolling mileage, obtained by least squares fitting method.

This friction coefficient model considers the two factors of rolling speed and rolling length, while reducing the sensitivity of the model to the speed when the speed is too large.

2.1.3. Deformation Resistance Model. According to the characteristics of the cold rolling production process, the deformation resistance of the cold rolling process is mainly related to the deformation speed, the deformation temperature, and the cumulative deformation degree. Among them, the cumulative deformation degree is the main factor affecting the deformation resistance of the material. Based on the data analysis of a large number of practical productions, the third-order polynomial model is chosen to predict the deformation resistance.

$$K = 1.15\sigma_s, \tag{6}$$

$$\sigma_s = a + b\varepsilon_{\sum}^1 + c\varepsilon_{\sum}^2 + d\varepsilon_{\sum}^3, \tag{7}$$

$$\varepsilon_{\sum} = \frac{1}{3}\frac{H - h_0}{H} + \frac{2}{3}\frac{h_1}{H}, \tag{8}$$

where K is the deformation resistance; σ_s is the yield stress of the strip; $\varepsilon_{\sum}$ is the cumulative degree of deformation of the rolled piece; H is the thickness of the raw material; and a, b, c, d are undetermined coefficients of the polynomial model.

2.1.4. Rolling Pass Model. The number of rolling passes can be determined by

$$n = Int\frac{\ln(h_i/H)}{\ln(1-\varepsilon_m)}, \tag{9}$$

where n is the number of rolling passes; ε_m is the maximum reduction rate; and h_i is the target thickness. For a single stand reversing cold rolling mill, $\varepsilon_m \le 40\%$.

2.1.5. Rolling Torque and Rolling Power. During normal rolling, the rolling torque M_F required by the roll is as follows:

$$M_F = Fl' + (\tau_b - \tau_f)R. \tag{10}$$

The rolling power of the motor is determined by the rolling torque and the rotational speed of the roll, which can be calculated by the following formula:

$$P = M_{\sum}\omega, \tag{11}$$

$$M_{\sum} = M_F/i + M_f + M_x \pm M_d, \tag{12}$$

where P is the rolling power of the motor; $M_{\sum}$ is the main motor total torque; ω is the angular velocity of the motor. M_f is the additional friction torque; M_x is the idling torque; M_d is dynamic torque; and i is gear ratio.

2.2. Objective Functions. To increase the utilization rate of machinery, equipment, and motors and improve the quality of rolling products, the load distribution of rolling schedule needs to be optimized according to different objectives. The objectives of optimization under different conditions are different, so it is necessary to establish objective functions under various conditions from different viewpoints.

2.2.1. Energy Consumption Objective Function. Due to the different reduction of each pass, the rolling energy consumption of each pass is also different. After optimizing the reduction of each pass, a set of load distribution schemes can always be found, so that the total energy consumption of each pass is the lowest. Therefore, the minimum energy consumption objective function is established as follows:

$$\min P_t = \sum_{i=1}^{n} P_i(\varepsilon_i). \tag{13}$$

where P_t is the total energy consumption of rolling; P_i is the rolling power of the i_{th} pass; n is the number of rolling passes; and ε_i is the reduction rate of the i_{th} pass.

2.2.2. Equal Power Margin Objective Function. To give full play to the performance of the rolling mill motor and improve the production efficiency of the rolling mill as much as possible, it is hoped that the rolling power of each pass has the same relative power margins. It means that not only the difference of rolling power between adjacent passes is desired to be minimized but also the difference of rolling power between a certain pass and other passes is desired to be minimized. Therefore, the objective function of equal power margin is constructed as follows:

$$S_i = \frac{P_r - P_i}{P_r}, \tag{14}$$

$$\min S = \sum_{i=1}^{n}\sum_{j>i}^{n}\left|S_i - S_j\right|, \tag{15}$$

where P_r is the rated power of the main motor; and S_i is the power margin factor of the i_{th} pass.

2.2.3. Good Flatness Objective Function. Good flatness means that under the condition of a certain roll-shape system, it is ensured that the section geometry of the rolling stock before and after rolling is similar. Considering that the main influence of the exit crown is the rolling force, the objective function can be written as [7]:

$$\min G = \sum_{i=1}^{n}(F_i - Fo_i)^2, \tag{16}$$

where F_i is the rolling force of the i_{th} pass; and Fo_i is the rolling force to make the best plate shape of the i_{th} pass.

2.3. Constraint Conditions. When optimizing the rolling schedule, it is necessary to constrain the technological parameters of each pass, so that the parameters of each pass are less than the maximum allowed by the equipment capacity and technological conditions. Constraint conditions include technological constraints and equipment constraints. The major technological constraints are as follows:

$$\begin{aligned} \varepsilon_{\min\, i} \le \varepsilon_i \le \varepsilon_{\max\, i}, \\ h_{\min\, i} \le h_i \le h_{\max\, i}, \\ v_{\min\, i} \le v_i \le v_{\max\, i}, \\ t_{\min\, i} \le t_i \le t_{\max\, i}, \end{aligned} \tag{17}$$

where $\varepsilon_{\min\, i}$, $\varepsilon_{\max\, i}$ are, respectively, the minimum and maximum reduction rates allowed for the i_{th} pass; h_i is the outlet thickness of the i_{th} pass; $h_{\min\, i}$, $h_{\max\, i}$ are, respectively, the minimum and maximum outlet thickness allowed for the i_{th} pass; v_i is the rolling speed of the i_{th} pass; $v_{\min\, i}$, $v_{\max\, i}$ are, respectively, the minimum and maximum rolling speed allowed for the i_{th} pass; t_i is the tensile stress of the i_{th} pass; and $t_{\min\, i}$, $t_{\max\, i}$ are, respectively, the minimum and maximum tensile stress allowed for the i_{th} pass.

The constraints of the rolling mill are as follows:

$$\begin{aligned} F_i \le F_{\max}, \\ P_i \le P_{\max}, \\ M_i \le M_{\max}, \end{aligned} \tag{18}$$

where F_i, P_i, M_i are, respectively, the rolling force, the total power and roll torque of the i_{th} pass; and $F_{\max}$, $P_{\max}$, $M_{\max}$

are, respectively, the maximum rolling force, the rated power of the motor and the maximum roll torque.

2.4. Multiobjective Optimization Model of Rolling Schedule. It can be seen from the above analysis that the process parameters related to the optimization of the rolling schedule can be obtained from the mathematical model of the rolling process through the reduction of each pass. Therefore, the reduction rate of each pass is selected as the variable of the optimization model. For the rolling production of single-stand cold rolling mills, more attention is paid to reducing production cost and improving production efficiency. For this reason, a multiobjective optimization model of rolling schedule for single-stand reversible cold rolling mill is constructed with minimum energy consumption and equal power margin as objective functions. The optimization model of rolling schedule based on two objective functions is as follows:

$$\begin{aligned} &\min F(X) = (f_1(X), f_2(X)), \\ &\quad s.t. \qquad\qquad g_i(X) \in \Omega \; i = 1, 2 \cdots, n, \end{aligned} \tag{19}$$

where $f_1(X)$ is the energy consumption objective function; $f_2(X)$ is the equal power margin objective function; X is the set of reduction ratios of each pass. $g_i(X)$ are the i_{th} constraint conditions.

3. Multiobjective Artificial Fish Swarm Algorithm

Aiming at the multiobjective optimization problem of rolling schedule, a solution strategy based on multiobjective artificial fish swarm algorithm (MOAFSA) is proposed. The basic artificial fish swarm algorithm (AFSA) is a single objective swarm intelligent optimization algorithm. The artificial fish swarm algorithm is improved into a multiobjective optimization algorithm by designing a fast search Pareto optimal solution method, constructing a Pareto optimal solution set method, designing an artificial fish state update method and a bulletin board maintenance strategy. In this section, the basic artificial fish swarm algorithm is introduced firstly. Next, the specific methods of each link of the multiobjective artificial fish swarm algorithm and the application steps in the optimization of the rolling schedule are introduced.

3.1. Review of AFSA. The basic idea of AFSA is searching for an optimal solution by simulating the preying behavior of artificial fish [19]. The artificial fish corresponds to the optimal solution of the optimization problem, the water area corresponds to the solution space of the optimization problem, and the food concentration corresponds to the objective function of the optimization problem. Some parameters of AFSA are defined as follows [20]. There are N artificial fishes in a D-dimensional space. The state vector of the i_{th} artificial fish is $X_i = [x_{i1}, x_{i2}, \cdots, x_{iD}]$, $i = 1, \cdots, N$, and $Y_i = f(X_i)$ is the food concentration of artificial fish. The distance from the i_{th} artificial fish to the j_{th} artificial fish is $d_{ij} = \|X_i - X_j\|$. δ, Visual, Step, L, N_f are, respectively, the congestion factor of artificial fish swarm, the perceived range of artificial fish, moving step of artificial fish, maximum preying time, and the number of artificial fish within the perceived range. The artificial fish mainly updates its state through four behaviors [21, 22]: preying, following, swarming, and random. The four behaviors are described as follows:

(1) Preying behavior: assuming that the current state of the artificial fish is X, a new state X_{next} is obtained firstly according to Equation (20) and Equation (21). Then, the food concentration functions Y and Y_{next} for X and X_{next} are calculated, respectively. Determining whether Y_{next} is superior to Y. If Y_{next} is superior to Y, X will be moved to X_{next} according to Equation (21). Otherwise, the new state of artificial fish will continue to be obtained according to Equation (20) and Equation (21). If the artificial fish acquires new states more than L times and Y_{next} is still worse than Y, the artificial fish performs random behavior

$$X' = X + \text{Visual} \cdot \text{rand}\,(), \tag{20}$$

$$X_{next} = X + \frac{X' - X}{X' - X} \cdot \text{step} \cdot \text{rand}\,(), \tag{21}$$

where rand () is the random number between 0-1; X_{next} is the next state of artificial fish

(2) Following behavior: assuming that the current state of the artificial fish is X, the optimal state of the artificial fish within the perceived range is X_{gbest}. If the food concentration X_{gbest} corresponding to Y_{gbest} is superior to Y, and $Y_{gbest}/N_f < \delta \bullet Y$, then, X moves to X_{gbest} according to Equation (22), otherwise the swarming behavior is performed as

$$X_{\text{next}} = X + \frac{X_{\text{gbest}} - X}{\left\| X_{\text{gbest}} - X \right\|} \bullet \text{step} \bullet \text{rand}\,() \tag{22}$$

(3) Swarming behavior: assuming that the current state of the artificial fish is X, the central position of the artificial fish within the perceived range is X_c. If the food concentration X_c corresponding to Y_c is superior to Y, and $Y_c/N_f < \delta \bullet Y$, then, X moves to X_c according to Equation (23), otherwise the preying behavior is performed as

$$X_{next} = X + \frac{X_c - X}{\|X_c - X\|} \bullet step \bullet \text{rand}\,() \tag{23}$$

(4) Random behavior: the artificial fish moves to a new state randomly according to Equation (20) within the perceived range

3.2. MOAFSA. According to the ideas of multiobjective evolutionary algorithm and multiobjective particle swarm algorithm [23–27], to improve the basic artificial fish swarm algorithm to multiobjective artificial fish swarm algorithm, the following three issues need to be addressed. (1) Fast searching Pareto optimal solutions and constructing Pareto optimal solution set; (2) determining the moving direction of artificial fish under multiobjective conditions; and (3) maintaining and updating the bulletin board (external archives) of artificial fish swarm.

(1) Fast searching Pareto optimal solutions and constructing Pareto optimal solution set

Searching for the Pareto optimal solution quickly and constructing the Pareto optimal solution set are the key points in multiobjective optimization problems [28]. Kong et al. proposed a method of fast searching for Pareto optimal solutions and constructing Pareto optimal solution set [29]. This method greatly improves the speed of searching for the Pareto optimal solution and the speed of constructing the Pareto optimal solution set, but it does not consider the situation of an existing multiple first objective functions with the same value when searching for the Pareto optimal solution. On the basis of this method, in this section, an improved method of fast searching Pareto optimal solutions and constructing Pareto optimal solution set is introduced [30]. According to the optimization problem required in this paper, the number of objective functions is defined as 2, and the optimization objective is to minimize the objective function. There are M total artificial fishes as alternative solutions. The steps of searching for Pareto optimal solutions and constructing Pareto optimal solution set are as follows:

(2) Status update of MOAFSA

Step 1. M alternative solutions are sorted rapidly in ascending order according to the first objective function; the sorted artificial fish are numbered 1 to M. At the same time, the artificial fishes with the same first objective function value are marked. The first alternative solution is selected temporarily as the Pareto optimal solution, and this alternative solution is added to the Pareto optimal solution set temporarily. Then, the second objective function of this alternative solution is set as the reference value, let $i = 2$.

Step 2. Determining whether the first objective function of the i_{th} artificial fish is the same as the first objective function corresponding to the current reference value, if it is the same, execute step 3, otherwise execute step 4.

Step 3. Compare the second function value of the i_{th} artificial fish with the reference value, if it is smaller than the reference value, remove this solution corresponding to the current reference value from the Pareto optimal solution set, and the i_{th} artificial fish is added to the Pareto optimal solution set temporarily, the second objective function value of this artificial fish is set as the reference value, and then, execute step 5, otherwise directly execute step 5.

Step 4. Compare the second function value of the i_{th} artificial fish with the reference value, if it is smaller than the reference value, and the i_{th} artificial fish is added to the Pareto optimal solution set temporarily, the second objective function value of this artificial fish is set as the reference value, and then, execute step 5, otherwise directly execute step 5.

Step 5. Let $i = i + 1$, determining whether i is greater than M, if i is greater than M, the comparison is stop, and the final, Pareto optimal solution sets are outputted, otherwise go to Step 2.

Since the Pareto optimal definition of the multiobjective optimization algorithm is introduced, the congestion factor δ of the AFSA is no longer applicable, and the congestion factor δ is replaced by defining a congestion distance Dis [31]. When determining the movement of the artificial fish, the congestion distance and the Pareto dominance rule are considered. After improvement, the status of artificial fish of the MOAFSA can be updated by the three behaviors of preying, following, and swarming.

Assuming that there are N_f artificial fish in the perceived range of the artificial fish, the steps for calculating the congestion distance Dis are as follows:

Step 1. The congestion distance of each artificial fish is initialized to 0, and the number of current objectives j is set to 1.

Step 2. The j_{th} objective is sorted in ascending order, and the sorted artificial fishes are remarked. Assuming that the i_{th} artificial fish is remarked as i', let the congestion distance of the artificial fish with $i' = 1$ and $i' = N_f$ be infinite, and let $i = 2$.

Step 3. The congestion distance of the i_{th} artificial fish is calculated according to .

$$Dis(i) = Dis(i) + \left| \frac{f_j\left(i' + 1\right) - f_j\left(i' - 1\right)}{\max\left(f_j\right) - \min\left(f_j\right)} \right|. \tag{24}$$

Step 4. Let $i = i + 1$, if $i > N_f$, go to step 5, otherwise go to step 3.

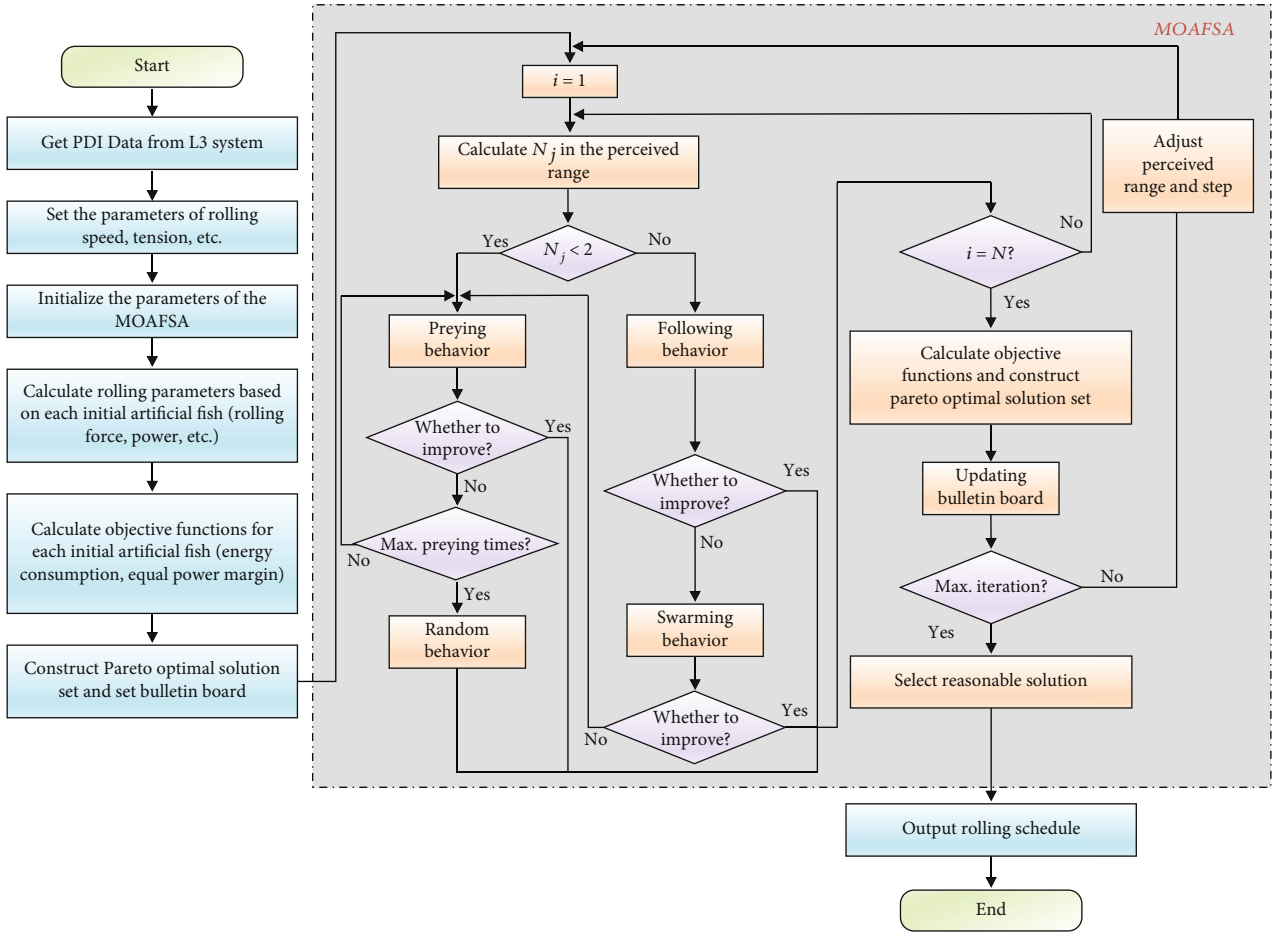

Figure 2: The flow chart of optimization of rolling schedule based on MOAFSA.

Step 5. Let $j = j + 1$, if $j > 2$, the final result is outputted and the calculation is stopped, otherwise go to step 2.

After the introduction of the Pareto dominance rule and the congestion distance, the three behaviors of preying, following, and swarming have also been improved accordingly. The specific improvements are as follows:

(a) Preying behavior: assuming that the current state of the artificial fish is X, a new state X_{next} is obtained firstly according to Equation (20) and Equation (21). Since the food concentration function is no longer a value, but a vector, the basis for determining whether X moves to X_{next} is whether $F(X_{next})$ dominates $F(X)$. If $F(X_{next})$ dominates $F(X)$, then, X moves to X_{next}, otherwise continue generating a new solution according to Equation (20) and Equation (21) until exceeding L times, and then, performs random behavior

(b) Following behavior: assuming that the current state of the artificial fish is X, the artificial fish searches for nondominated solutions within its perceived range according to the Pareto dominance rule, then, calculate the congestion distance of each artificial fish is calculated, and the solution X_{gbest} with the largest congestion distance is obtained. If $Dis(X_{gbest}) < Dis(X)$, X moves to X_{gbest} according to Equation (22), otherwise the swarming behavior is performed

(c) Swarming behavior: assuming that the current state of the artificial fish is X, the central position of the artificial fish within the perceived range is X_c. If $F(X_c)$ dominates $F(X)$ and $Dis(X_c) < Dis(X)$, X moves to X_c according to Equation (23), otherwise the preying behavior is performed

(3) Maintenance strategy of bulletin board for MOAFSA

In the AFSA, the bulletin board is used to record the position of the optimal artificial fish and the food concentration function in each iteration process. With the introduction of Pareto optimal definition in multiobjective optimization, the bulletin board no longer only records the position and food concentration function of an artificial fish, but it is equivalent to the external file set of multiobjective evolutionary algorithm and multiobjective particle swarm optimization algorithm, and becomes Pareto optimal

solution set [32]. Therefore, the maintenance and update of the bulletin board is a necessary link for the artificial fish to obtain a Pareto front with better diversity and distribution when moving. In this paper, the maintenance strategy based on grid density commonly used in multiobjective evolutionary algorithm and multiobjective particle swarm algorithm is adopted [29]. When the bulletin board is updating, the Pareto optimal solution set obtained in this iteration process is merged with the bulletin board firstly, and the dominated artificial fish is eliminated according to the above method. Then, determine whether the number of artificial fish in the bulletin board is greater than the maximum number of artificial fish K_m in the bulletin board. If it is greater than K_m, the target space of each dimension of the bulletin board is divided into 10 parts equally; then, the entire target space is evenly divided into 100 blocks. The number of all artificial fish in the area where each artificial fish is located is defined as the grid density of this artificial fish, and finally, the artificial fish with the largest grid density is removed one by one until the number of artificial fish is equal to K_m.

Therefore, the implementation steps of the MOAFSA are summarized as follows:

$$\phi = \exp\left(-30 \bullet \left(\frac{t}{T)^{10}}\right)\right), \tag{25}$$

$$\text{Step} = \text{Step} \bullet \phi + \text{Step}_{\min}, \tag{26}$$

$$\text{Visual} = \text{Visual} \bullet \phi + \text{Visual}_{\min}. \tag{27}$$

Step 1. Initializing all parameters of the MOAFSA.

Step 2. Calculating the objective functions, searching for the Pareto optimal solution, and constructing the Pareto optimal solution set, and the Pareto optimal solution set is merged with the bulletin board.

Step 3. Calculating the number of other artificial fish N_f in the perceived range of each artificial fish, if $N_f < 2$, executing preying behavior, otherwise execute the following behavior.

Step 4. Calculating the objective functions, searching for the Pareto optimal solution, and constructing the Pareto optimal solution set of this iteration process, and the Pareto optimal solution set is merged with the bulletin board.

Step 5. To improve the convergence speed and convergence accuracy, the perceived range and moving step of artificial fish are updated according to, [33] and are as follows:

Step 6. Determining whether the number of iterations is greater than the maximum number of iterations T, if it is greater than T, outputting the bulletin board, and outputting the artificial fish with the smallest grid density as the optimal solution, otherwise go to Step 3.

3.3. MultiObjective Optimization Process of Rolling Schedule Based on MOAFSA. MOAFSA will be applied to the optimization of rolling schedule to search a load distribution scheme which considers two objectives. First, the product specification to be optimized needs to be obtained, which is usually obtained from the L3 production management system. Second, according to finished product specifications, the production constraints are set, such as tension limit values, and rolling speed limits. Then, the parameters of the MOAFSA are initialized, and the initial value of rolling parameters and the initial value of the objective function are calculated. After that, the iterative process of MOAFSA is entered, and the result of load distribution is obtained after reaching the maximum number of iterations. The detailed optimization flow of the rolling schedule based on MOAFSA is shown in Figure 2.

Table 1: Mechanical and electrical parameters of the rolling mill.

Parameters	Value
Power [KW]	6000
Max. Rolling force [KN]	12000
Max. Rolling speed [m/min]	1300
Max. Diameter of work roll [mm]	397
Mill rigidity coefficient [KN/mm]	3500
Max. Tension [KN]	170

4. Engineering Implementation and Validation

In the practical cold rolling project, the optimization of the rolling schedule is realized in the L2 process automation system. After the L2 process automation system receives the production plan and raw material information from the L3 production management system, the rolling technological table consisting of a set of detailed basic automation settings according to the rolling process mathematical model and the rolling schedule optimization method is calculated. According to the control sequence, the rolling technological table of the corresponding raw material is sent to the basic automation level for precise control. In this section, to verify the validity and feasibility of the rolling schedule optimization method based on MOAFSA in the practical system, the proposed method was tested in the practical system and compared with the rolling schedule based on experience.

4.1. Description of Plant. The platform of the verification experiment adopts the self-developed 1380 mm single-stand six-high reversible cold rolling mill automation system. The automation system adopts a two-level automation control system structure, which consists of a process automation system (L2) and a basic automation system (L1). And the system has a communication interface with production management automation system (L3), which can communicate with the L3 in real time. The rolling mill equipment uses two independent hydraulic cylinders to generate rolling force, and the rolls are driven by AC motors. The mechanical and electrical parameters of the rolling mill

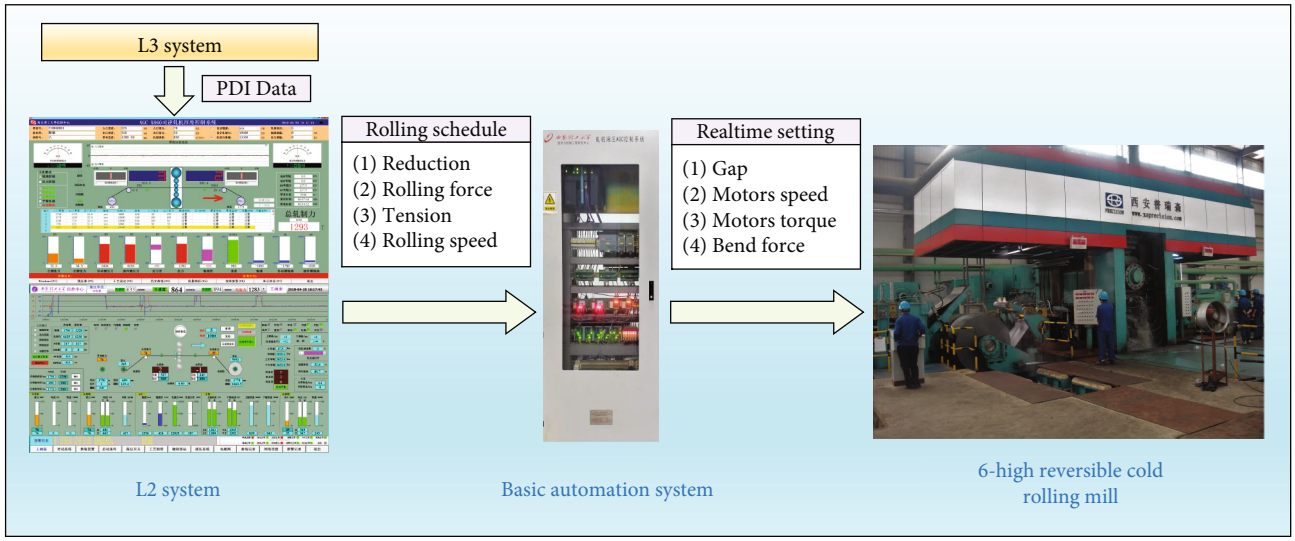

Figure 3: Single stand reversible cold rolling mill and automa1tion system.

Table 2: Parameters and production requirements of the tested steel coils.

Parameters	No.1 SPEC.	No.2 SPEC.
Steel grade	SPHC	Q195
Width [*mm*]	1075	1225
Weight [*T*]	19.35	22.05
Initial thickness [*mm*]	2.75	3
Target thickness [*mm*]	0.16	0.25
Total pass	6	6

are shown in Table 1. The practical rolling mill and automation system are shown in Figure 3.

4.2. Experimental Results and Analysis. To verify the rolling schedule optimization method proposed in this paper, two product specifications with the largest output selected from the product outline of this cold rolling mill were tested, respectively. The specific parameters and production requirements of these two product specifications are shown in Table 2. For No.1 SPEC., the optimal rolling schedule and the empirical rolling schedule use the same tension coefficient and rolling speed. For No.2 SPEC., the optimal rolling schedule and the empirical rolling schedule use the same tension coefficient, but the rolling speed is set according to the limit of rolling power and the maximum speed of motor. The rolling schedules obtained by both methods are sent to the basic automation system for production, and the application effects of the rolling schedules are compared through the collected practical production data.

According to the rolling characteristics, the reduction ratios of each pass were randomly generated within a reasonable range to constitute the initial position of the artificial fishes. The initial value of Step is 0.02. The initial state of the bulletin board is empty. The other parameters of MOAFSA are as follows:

(1) The number of artificial fishes N: 30

(2) The maximum preying time L: 10

(3) The perceived range of artificial fish Visual: 0.05

(4) The minimum perceived range of artificial fish $\text{Visual}_{\min}$: 0.01

(5) The minimum moving step of artificial fish $\text{Step}_{\min}$: 0.005

(6) The maximum number of iterations T: 100

(7) The maximum number of bulletin boards K_m: 100

Taking the minimum energy consumption and equal power margin as the objective function, the approximate Pareto optimal solution set after the normalization of the two specifications is obtained through the optimization calculation, as shown in Figure 4.

The optimization method proposed in this paper is repeated independently for 20 times, and the experimental results are taken as the average value of the 20 experiments. The artificial fish with the smallest lattice density was selected as the optimal solution and sent to the basic automation system for production. Tables 3 and 4 show the comparison of the load distribution and practical production data of the two specifications of strip with the optimized rolling schedule and the empirical rolling schedule.

The power distribution of each pass of two specifications based on empirical and optimized method is shown in Figure 5.

Figure 5(a) shows the power distribution of No.1 SPEC., compared with the empirical rolling schedule, the total energy consumption of the rolling schedule obtained by the proposed method is almost the same as that of the

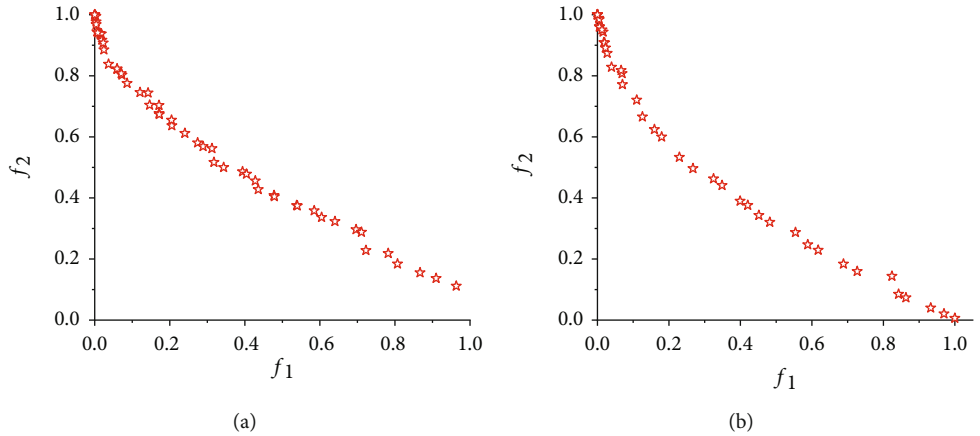

Figure 4: Pareto optimal set. (a) No.1 SPEC. (b) No.2 SPEC.

Table 3: Comparison of optimized schedule (Opt.) and empirical schedule (Emp.) for No.1 SPEC.

Pass	Method	Outlet thickness [mm]	Reduction rate	Rolling force [KN]	Power [KW]	Rolling speed [m/min]	Rolling time [min]
1	Opt.	1.73	0.37091	8242	4449	500	2.932
	Emp.	1.92	0.30	6550	3184	500	2.67
2	Opt.	1.07	0.38150	8521	4618	600	3.909
	Emp.	1.16	0.395	8967	5169	600	3.632
3	Opt.	0.65	0.39252	8636	4609	700	5.433
	Emp.	0.70	0.395	8807	4870	700	5.073
4	Opt.	0.390	0.40	8749	4566	800	7.799
	Emp.	0.42	0.40	8717	4650	800	7.274
5	Opt.	0.235	0.39744	8396	4713	1000	10.32
	Emp.	0.255	0.39	8177	4631	1000	9.554
6	Opt.	0.16	0.31915	8717	5150	1200	12.617
	Emp.	0.16	0.37	9342	5856	1200	12.615

empirical rolling schedule, but the proposed method can obtain a more uniform power distribution. The power margins of the empirical rolling schedule and the optimized rolling schedule are 1.1530 and 0.0053, respectively, which means that the optimized rolling schedule still has the potential to increase the rolling speed in the middle several passes, which can further improve the production efficiency. To verify the ability of the proposed algorithm in improving productivity, during the production of the No.2 SPEC, the rolling speed is only limited by the motor power and the maximum rotate speed, regardless of the experience rolling schedule or the optimized rolling schedule. Figure 5(b) shows a comparison of the power distribution for the empirical and optimized rolling schedules of the No.2 SPEC. The power margins of the empirical rolling schedule and the optimized rolling schedule are 0.9910 and 0.4884, respectively. It can be seen from Figure 5(b) that the two design methods of rolling schedule try to maximize the power capability of the motor, compared with the empirical rolling schedule, the power distribution of each pass of the optimized rolling schedule is more uniform, and the rolling power of more passes can approach the limit value of the rolling power. It means that the optimized rolling schedule can better utilize capacity of the rolling mill. Figure 6 shows the comparison of the rolling efficiency for the No.2 SPEC between the optimized rolling schedule and the empirical rolling schedule.

Figure 6(a) shows the comparison of rolling speed for No.2 SPEC. It can be clearly seen from Figure 6(a) that the rolling speed of the optimized rolling schedule has been significantly improved in the middle three passes, and the production efficiency has been significantly improved. Figure 6(b) shows the comparison of rolling time, which also confirms the advantages of the optimized rolling schedule in improving the production efficiency in the middle three passes. Using the optimized rolling schedule, the production time of each coil can save 1.308 min, which is also a very meaningful improvement for mass production. As shown

Table 4: Comparison of optimized schedule (Opt.) and empirical schedule (Emp.) for No.2 SPEC.

Pass	Method	Outlet thickness [mm]	Reduction rate	Rolling force [KN]	Power [KW]	Rolling speed [m/min]	Rolling time [min]
1	Opt.	2.01	0.33	8493	4496	500	2.563
	Emp.	2.10	0.30	7663	3866	500	2.465
2	Opt.	1.33	0.33831	8770	5876	740	2.764
	Emp.	1.37	0.35	9284	5897	678	2.850
3	Opt.	0.87	0.34586	8738	5831	860	3.548
	Emp.	0.87	0.36	9429	5868	770	3.856
4	Opt.	0.60	0.31034	7761	5876	1200	3.859
	Emp.	0.56	0.36	8598	5894	1020	4.588
5	Opt.	0.39	0.35	8246	5829	1200	5.839
	Emp.	0.37	0.34	8100	5540	1200	6.519
6	Opt.	0.25	0.35897	8779	5644	1200	8.220
	Emp.	0.25	0.32	8279	5054	1200	8.318

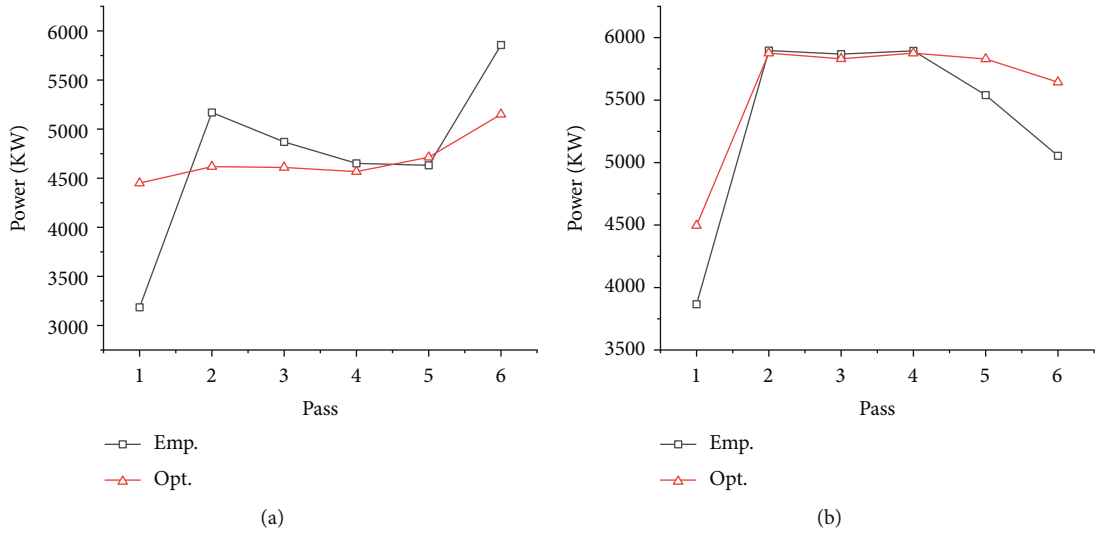

Figure 5: Power distribution of the two methods. (a) No.1 SPEC. (b) No.2 SPEC.

in Figure 7, the total power consumption of the rolling schedule obtained by the optimized method is almost the same as that of the empirical rolling schedule, which is also determined by the production characteristics of the single-stand cold rolling mill.

However, the empirical rolling schedule design method does not consider the influence of changes in production parameters, and the results on production efficiency are completely unknown. In applying the empirical rolling schedule, the operator needs to modify the technological setting parameters repeatedly, which is easy to cause unstable product quality and affect production efficiency. The significance of the optimization method of rolling schedule based on MOAFSA is that the setting value of technological parameter which takes into account some objectives can be automatically calculated without relying on personal experience. In practical application, compared with the empirical rolling schedule, the operator does not need to modify the technological setting parameters frequently, the product quality is more stable, and the production efficiency is higher. When the production parameters change, the results of the optimized rolling schedule will change accordingly, i.e., the optimization method of rolling schedule based on MOAFSA has better adaptability. As can be seen from the above experimental results, the optimization method of rolling schedule based on MOAFSA can obtain a result that takes into account the total rolling power consumption and rolling efficiency, and can effectively improve the production efficiency without consuming too much power consumption. The experimental results also show the feasibility and effectiveness of the proposed algorithm.

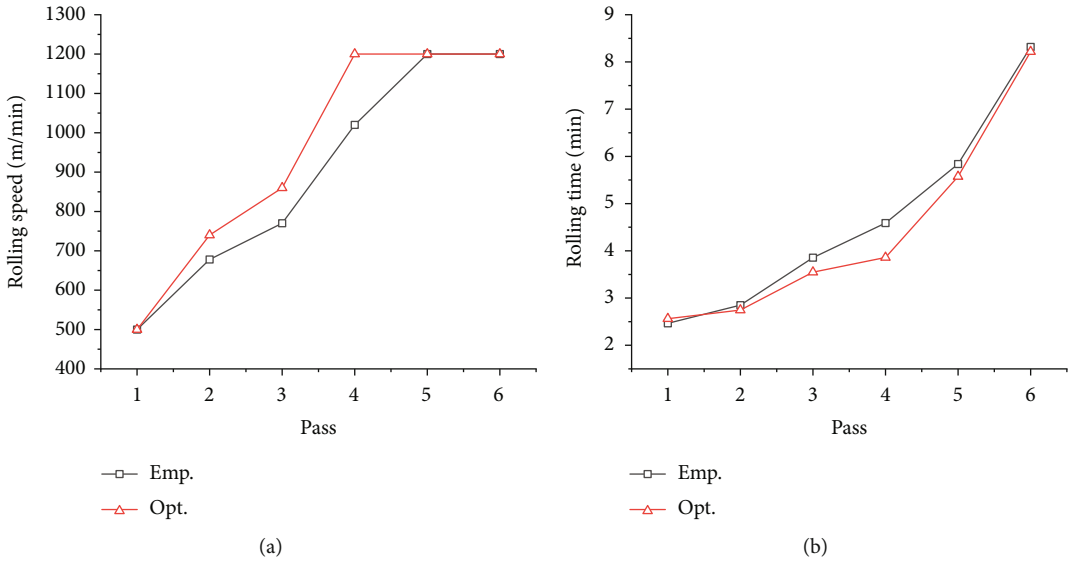

Figure 6: The comparison of rolling efficiency for NO.2 SPEC. (a) Rolling speed comparison. (b) Rolling time comparison.

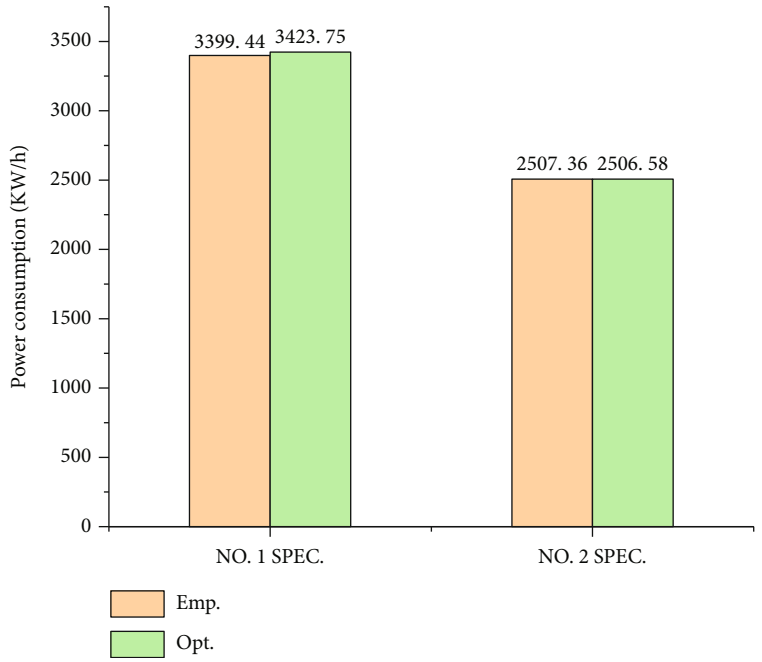

Figure 7: The comparison of rolling power consumption.

5. Conclusions

In this work, a rolling schedule optimization method based on MOASFA was proposed for the single-stand reversible cold rolling process. First, a multiobjective optimization model composed of an energy consumption function and equal power margin function was designed, and these objective functions were calculated based on the proposed mathematical model of the rolling process of single-stand cold rolling mill suitable for practical engineering applications. Then, the AFSA was improved into a multiobjective optimization method, and the method of quickly constructing Pareto optimal solution set was improved. At the same time, the four behaviors of artificial fish are improved under the framework of multiobjective optimization, and the maintenance strategy for the bulletin board of artificial fish swarm algorithm in the multiobjective optimization algorithm is added. The practical industrial verification of rolling scheduling optimization based on MOASFA proves the effectiveness and feasibility of the proposed algorithm. On the basis of roughly the same energy consumption, the rolling schedule optimization method proposed in this paper can

improve the production efficiency by 4.6% compared with the experience rolling schedule. This study provides a useful exploration for the application of optimized rolling schedules in practical engineering. When there are many objective functions, the method of constructing Pareto optimal solution set adopted in this paper still has high algorithm complexity, which limits the introduction of more objective functions. Therefore, it is necessary to further study the method of rapidly constructing Pareto optimal solution set. At the same time, more objective functions will be introduced in the optimization of rolling schedule.

Data Availability

The data used to support the findings of this study are available from the corresponding author upon request.

Conflicts of Interest

The authors declare that they have no conflict of interest.

Acknowledgments

This work was supported by the National Natural Science Foundation (NNSF) of China [grant numbers 62003261 and 62073258].

References

[1] Z. Hu, Z. Wei, H. Sun, J. Yang, and L. Wei, "Optimization of metal rolling control using soft computing approaches: a review," *Archives of Computational Methods in Engineering*, vol. 28, no. 2, pp. 405–421, 2021.

[2] I. Imai, "Continuous rolling theory in hot strip mill and its application," *Bulletin of JSME*, vol. 7, no. 26, pp. 430–436, 1964.

[3] M. Kamata, *Continuous Rolling of Sheet Products Footsteps of Engineers Who Have Persued the world's Most Advanced Technology*, Metallurgical Industry Press, Beijing, 2002.

[4] K. Sekiguchi, Y. Seki, N. Okitani et al., "The advanced set-up and control system for Dofasco's tandem cold mill," *IEEJ Transactions on Industry Applications*, vol. 32, no. 3, pp. 608–616, 1996.

[5] H. Li, J. Xu, G. Wang, and X. H. Liu, "Improvement on conventional load distribution algorithm in hot tandem mills," *Journal of Iron and Steel Research International*, vol. 14, no. 2, pp. 36–41, 2007.

[6] J. Sheng, Z. Jiao, and G. Wang, "Simple iteration method of calculating load distribution for reversible cold mill," *Journal of Iron and Steel Research*, vol. 19, no. 3, pp. 35–37, 2007.

[7] X. Jin, C. Li, Y. Wang, X. Li, Y. Xiang, and T. Gu, "Investigation and optimization of load distribution for tandem cold steel strip rolling process," *Metals - Open Access Metallurgy Journal*, vol. 10, no. 5, p. 677, 2020.

[8] Y. Cao, J. Cao, T. Wang et al., "The cold rolling load distribution of the nuclear power zirconium alloy based on the self-adaptive particle swarm optimization algorithm," *The International Journal of Advanced Manufacturing Technology*, vol. 119, no. 9-10, pp. 6007–6016, 2022.

[9] J. Yang, C. Wang, H. Che, and L. Zhao, "Improved ABC algorithm based on aluminum hot strip mill rolling schedule optimization design," *Journal of Plasticity Engineering*, vol. 20, no. 5, pp. 91–96, 2013.

[10] S. Chen, X. Zhang, L. G. Peng, D. H. Zhang, J. Sun, and Y. Z. Liu, "Multi-objective optimization of rolling schedule based on cost function for tandem cold mill," *Journal of Central South University*, vol. 21, no. 5, pp. 1733–1740, 2014.

[11] H. N. Bu, Z. W. Yan, D. H. Zhang, and S. Z. Chen, "Rolling schedule multi-objective optimizationbased on influence function for thin gauge steel strip in tandem cold rolling," *Scientia Iranica*, vol. 23, no. 6, pp. 2663–2672, 2016.

[12] Y. Wang, C. Li, X. Jin, Y. Xiang, and X. Li, "Multi-objective optimization of rolling schedule for tandem cold strip rolling based on NSGA-II," *Journal of Manufacturing Processes*, vol. 60, pp. 257–267, 2020.

[13] H. Che, L. Wang, J. Gu, L. Huo, H. Sun, and J. Yang, "Rolling schedule optimization based on adaptive grid multi-objective quantum genetic algorithm," *Journal of Plasticity Engineering*, vol. 23, no. 6, pp. 79–86, 2016.

[14] Y. Li and L. Fang, "Robust multi-objective optimization of rolling schedule for tandem cold rolling based on evolutionary direction differential evolution algorithm," *Journal of Iron and Steel Research International*, vol. 24, no. 8, pp. 795–802, 2017.

[15] L. Wei, L. Wang, M. Ma, H. Che, and J. Yang, "Optimization of tandem cold rolling schedule based on improved multi-objective particle swarm optimization algorithm," *China Mechanical Engineering*, vol. 26, no. 9, pp. 1239–1242, 2015.

[16] Y. Wang, J. Wang, C. Yin, and Q. Zhao, "Multi-objective optimization of rolling schedule for five-stand tandem cold mill," *IEEE Access*, vol. 8, pp. 80417–80426, 2020.

[17] Z. Hu, Z. Wei, X. Ma, H. Sun, and J. Yang, "Multi-parameter deep-perception and many-objective autonomous-control of rolling schedule on high speed cold tandem mill," *ISA Transactions*, vol. 102, pp. 193–207, 2020.

[18] Z. Babajamali, M. K. khabaz, F. Aghadavoudi, F. Farhatnia, S. A. Eftekhari, and D. Toghraie, "Pareto multi-objective optimization of tandem cold rolling settings for reductions and inter stand tensions using NSGA-II," *ISA Transactions*, 2022.

[19] X. L. Li, Z. J. Shao, and J. X. Qian, "An optimizing method based onautonomous animats: fish-swarm algorithm," *Institute of Sy stems Engineering*, vol. 11, pp. 32–38, 2002.

[20] J. Huang, J. Zeng, Y. Bai et al., "Layout optimization of fiber Bragg grating strain sensor network based on modified artificial fish swarm algorithm," *Optical Fiber Technology*, vol. 65, article 102583, 2021.

[21] Y. Zhu, W. Xu, G. Luo, H. Wang, J. Yang, and W. Lu, "Random forest enhancement using improved artificial fish swarm for the medial knee contact force prediction," *Artificial Intelligence In Medicine*, vol. 103, article 101811, 2020.

[22] Y. Gao, L. Xie, Z. Zhang, and Q. Fan, "Twin support vector machine based on improved artificial fish swarm algorithm with application to flame recognition," *Applied Intelligence*, vol. 50, no. 8, pp. 2312–2327, 2020.

[23] K. Alkebsi and W. L. Du, "A fast multi-objective particle swarm optimization algorithm based on a new archive updating mechanism," *IEEE Access*, vol. 8, pp. 124734–124754, 2020.

[24] J. Meza, H. Espitia, C. Montenegro, and R. G. Crespo, "Statistical analysis of a multi-objective optimization algorithm based on a model of particles with vorticity behavior," *Soft Computing*, vol. 20, no. 9, pp. 3521–3536, 2016.

[25] M. L. Yang, Y. M. Liu, and J. Yang, "A hybrid multi-objective particle swarm optimization with central control strategy," *Computational Intelligence and Neuroscience*, vol. 2022, Article ID 1522096, 23 pages, 2022.

[26] Z. Liu, Z. Qin, P. Zhu, and H. Li, "An adaptive switchover hybrid particle swarm optimization algorithm with local search strategy for constrained optimization problems," *Engineering Applications of Artificial Intelligence*, vol. 95, article 103771, 2020.

[27] H. F. Wang, Y. P. Fu, M. Huang, G. Huang, and J. W. Wang, "A hybrid evolutionary algorithm with adaptive multi-population strategy for multi-objective optimization problems," *Soft Computing*, vol. 21, no. 20, pp. 5975–5987, 2017.

[28] X. Y. Zhang, X. T. Zheng, R. Cheng, J. Qiu, and Y. Jin, "A competitive mechanism based multi-objective particle swarm optimizer with fast convergence," *Information Sciences*, vol. 427, pp. 63–76, 2018.

[29] W. Kong, T. Chai, J. Ding, and Z. Wu, "A real-time multiobjective electric energy allocation optimization approach for the smelting process of magnesia," *Acta Automatica Sinica*, vol. 30, no. 1, pp. 51–61, 2014.

[30] D. Liu, X. Zhang, and Y. Chen, "Monocrystalline silicon diameter detection image threshold segmentation method using multi-objective artificial fish swarm algorithm," *Acta Automatica Sinica*, vol. 42, no. 3, pp. 431–442, 2016.

[31] Z. Zhang, K. Wang, L. Zhu, and Y. Wang, "A Pareto improved artificial fish swarm algorithm for solving a multi-objective fuzzy disassembly line balancing problem," *Expert Systems with Applications*, vol. 86, pp. 165–176, 2017.

[32] Y. Liu, X. Feng, L. Zhang, W. Hua, and K. Li, "A Pareto artificial fish swarm algorithm for solving a multi-objective electric transit network design problem," *Transportmetrica A: Transport Science*, vol. 16, no. 3, pp. 1648–1670, 2020.

[33] X. Zhang, L. Lian, and F. Zhu, "Parameter fitting of variogram based on hybrid algorithm of particle swarm and artificial fish swarm," *Future Generation Computer Systems*, vol. 116, no. 1, pp. 265–274, 2021.